Journal of Power Sources 196 (2011) 7835–7840

Contents lists available at ScienceDirect

Journal of Power Sources

journal homepage: www.elsevier.com/locate/jpowsour

Growth of polyaniline nanowhiskers on mesoporous carbon for supercapacitor application

Yanfang Yan [a], Qilin Cheng [a,b,*], Gengchao Wang [a], Chunzhong Li [a,*]

[a] Key Laboratory for Ultrafine Materials of Ministry of Education, School of Materials Science and Engineering, East China University of Science and Technology, 200237 Shanghai, China

[b] Centre of Polymer Systems, Polymer Centre, Tomas Bata University in Zlin, nam. T. G. Masaryka 5555, 760 01 Zlin, Czech Republic

ARTICLE INFO

Article history:
Received 13 January 2011
Received in revised form 17 March 2011
Accepted 29 March 2011
Available online 5 April 2011

Keywords:
Polyaniline nanowhiskers
Mesoporous carbon
Nanocomposite
Electrochemical properties

ABSTRACT

Vertically aligned polyaniline nanowhiskers (PANI-NWs) doped with (1R)-(−)-10-Camphorsulfonic acid (L-CSA) have been successfully synthesized on the external surface of ordered mesoporous carbon (CMK-3) by chemical oxidative polymerization. The specific surface area of the PANI-NWs/CMK-3 nanocomposite remains as high as 497 $m^2 g^{-1}$ by removing mesoporous silica template after the polymerization of aniline. Structural and morphological characterizations of the nanocomposite were further investigated by XRD, FTIR and FE-SEM measurements. The result shows that the nanocomposite with 40 wt% PANI applying in supercapacitor devices possesses a large specific capacitance of 470 $F g^{-1}$ and good capacitance retention of 90.4% is achieved after 1000 cycles at a current density of 1.0 $A g^{-1}$. The synergistic effect of small PANI nanowhisker arrays and well-ordered mesoporous carbon endows the composite with high electrochemical capacitance and good cycling stability.

1. Introduction

With the increasing demand for powering systems of portable electronic devices and hybrid electric vehicles, researches on supercapacitor, a relatively new electrochemical energy storage device, have attracted enormous scientific interests because of its high power capability and long cycle life [1]. According to the charge-storage mechanism, supercapacitors can be divided into electrical double-layer capacitor (EDLC) and pseudo-capacitor [2]. In the case of EDLCs, energy storage is the accumulation of ionic charges which occur at the interface between the electrode and electrolyte [3,4]. Porous carbons as typical EDLC electrodes can provide high power density but much lower energy density than pseudocapacitor [5]. On the other hand, the pseudocapacitance is produced by the fast reversible faradic transitions of active materials, e.g., transition metal oxides, conducting polymers. Among these materials, PANI is a potential electrode material in redox supercapacitors because of its low cost, high conductivity and easy synthesis [6–8]. However, a pure electrode of PANI has drawbacks of poor cycling stability and temperature dependence.

Considering the practical applications, nanocomposites of carbon and conducting polymers have attracted much attention due to the synergistic effects between these components in recent years. CMK-3, a highly ordered hexagonally structured mesoporous carbon discovered by Ryoo's group [9], was demonstrated experimentally that it possessed superior capacitive performances than conventional carbon materials [10–13]. Therefore, many efforts have been devoted to prepare conducting polymer/mesoporous carbon nanocomposites [14–19] which can combine the advantages of the high power of EDLCs and the high specific energy of pseudocapacitors. More studies have also proved that these nanocomposites exhibit much higher capacitance value than individual components. However, the above-mentioned nanocomposites are almost obtained by direct polymerization of monomer on the mesoporous carbon, which inevitably leads to a significant decrease in the specific surface area of the resultant composite. For instance, Wang et al. [20] reported that PANI/CMK-3 nanocomposite in which whisker-like PANI on the surface of CMK-3 showed excellent capacitance (900 $F g^{-1}$), but its surface area decreased tremendously from 1300 $m^2 g^{-1}$ to 35 $m^2 g^{-1}$ as the mesopores were filled with PANI, and thus the electric double-layer capacitance of CMK-3 could not be utilized sufficiently.

Recently, nanostructured conducting polymers, which provide relatively shorter ions diffusion path than bulk ones, exhibited improved performance in energy storage [21,22]. In particular, aligned nanowire or nanotube arrays of conducting polymers used as electrode materials are found to be especially advantageous for supercapacitors. Kuila et al. [23] reported that vertically oriented PANI nanorods exhibited excellent electrochemical properties with a large capacitance value of 3407 $F g^{-1}$ but a poor cycling stability. In order to obtain materials with high capacitive performance and good cycle life, researchers are striving to develop nanocomposites

* Corresponding author. Tel.: +86 21 64250949; fax: +86 21 64250624.
E-mail addresses: chengql@ecust.edu.cn (Q. Cheng), czli@ecust.edu.cn (C. Li).

0378-7753/$ – see front matter © 2011 Elsevier B.V. All rights reserved.
doi:10.1016/j.jpowsour.2011.03.088

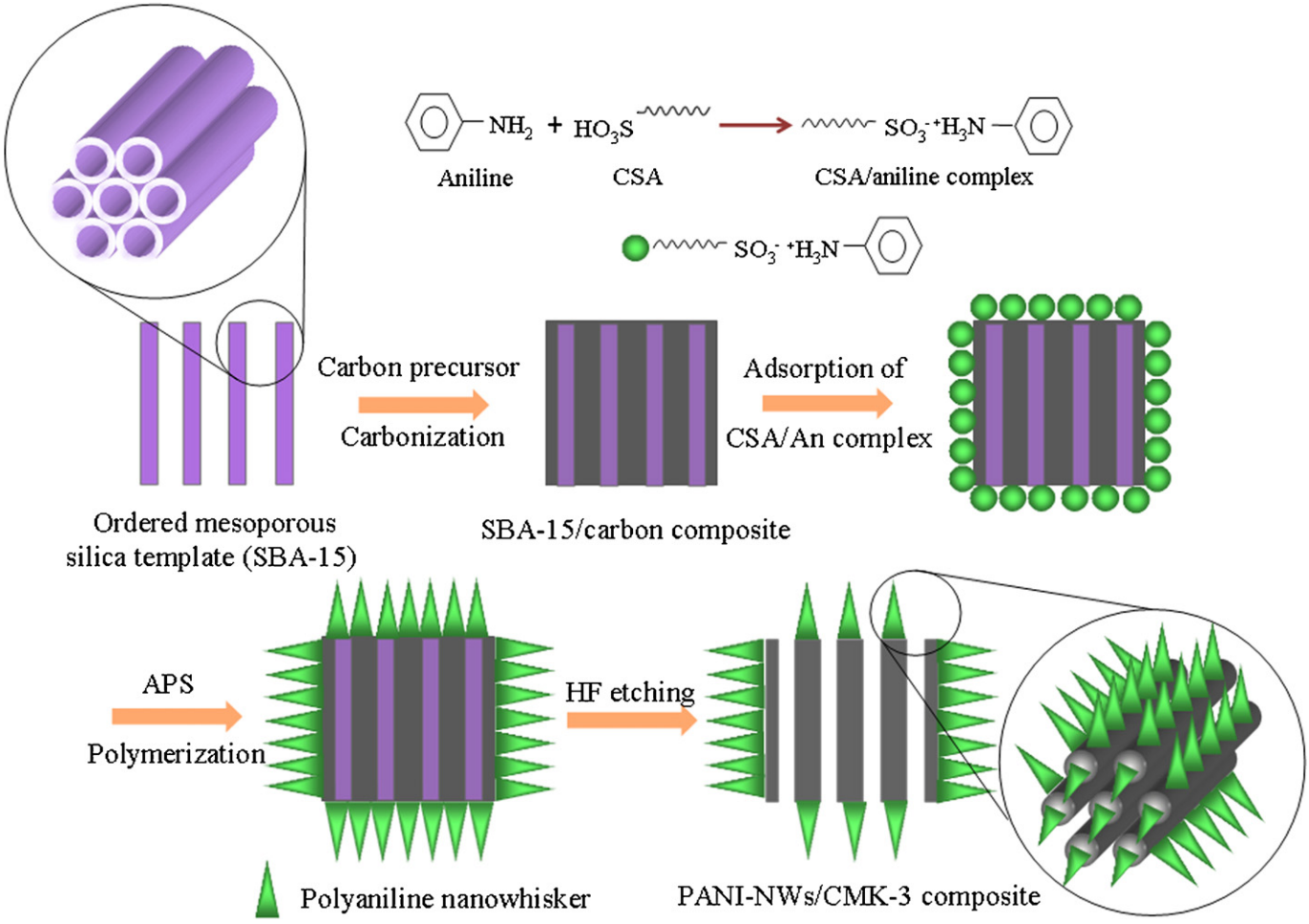

Fig. 1. Schematic illustration of the preparation process of PANI-NWs/CMK-3 nanocomposite.

consisting of one-dimensional conducting polymers with carbon materials [24]. However, there has been no report dealing with high surface area composite of nanostructured conducting polymer on mesoporous carbon so far.

Herein, we developed a simple approach to prepare a novel nanocomposite with PANI-NWs grown vertically on the outer surface of CMK-3 particles. PANI-NWs were formed on CMK-3 via chemical oxidative polymerization in the presence of CSA which acts as both dopant and structure-directing agent. The resulting composite can maintain ordered mesoporous structure and high surface area. The morphology, structure and electrochemical properties of the nanocomposite were investigated. The PANI-NWs/CMK-3 nanocomposite electrode for supercapacitors showed enhanced specific capacitance and cycling stability.

2. Experimental

2.1. Materials

Aniline (An, analytical grade) purchased from Shanghai Chemical Reagent Co. was distilled under vacuum prior to use. (1R)-(−)-10-Camphorsulfonic acid (CSA, 98%) and polytetrafluoroethylene (PTFE, 60 wt% dispersion in water) were supplied by Sigma Aldrich. Carbon black was obtained from TIMCAL Co., Swiss. Ammonium persulfate (APS, $(NH_4)_2S_2O_8$, 98%), hydrofluoric acid (HF, 40%) and other reagents were of analytical grade and used as received without further purification.

2.2. Synthesis of PANI/CMK-3 nanocomposite

The overall synthetic procedure of the PANI-NWs/CMK-3 composite was outlined in Fig. 1. CMK-3 particles serving as the backbone were selectively functionalized with aligned PANI-NWs and the internal mesopores could be preserved intact. Mesoporous silica (SBA-15) was synthesized according to the previous report [25] and used as the template to prepare a SBA-15/carbon composite by impregnating SBA-15 with sucrose and H_2SO_4 solution and then carbonizing the sucrose at 900 °C [9,26]. PANI-NWs/CMK-3 composite was then obtained by polymerization of aniline at 0–5 °C. In a typical procedure, 0.3 g of SBA-15/carbon powder were immersed in 10 ml aqueous solution containing 1×10^{-3} mol CSA and the mixture was ultrasonicated for 30 min. Afterwards, 2×10^{-3} mol aniline was added into the above solution at 0–5 °C and stirred for 30 min to form a uniform mixture. Then 5 ml precooled APS solution (the molar ratio of aniline/APS is 1) was added drop by drop while stirring to initiate the reaction. The mixture was allowed to react for 20 h with continuous stirring in the ice bath. The PANI-covered SBA-15/carbon composites were washed with 5% hydrofluoric acid solution to remove SBA-15 silica templates. Finally, the black-green resulting products were filtered and washed repeatedly with de-ionized water and alcohol, and then dried under vacuum at 50 °C for 24 h. In addition, PANI/CMK-3 composite was also prepared in the absence of CSA under the same conditions for comparison. The PANI content in both composites evaluated by calculating the weight increase of CMK-3 was 40 wt%. The PANI/CMK-3 without CSA and CSA doped

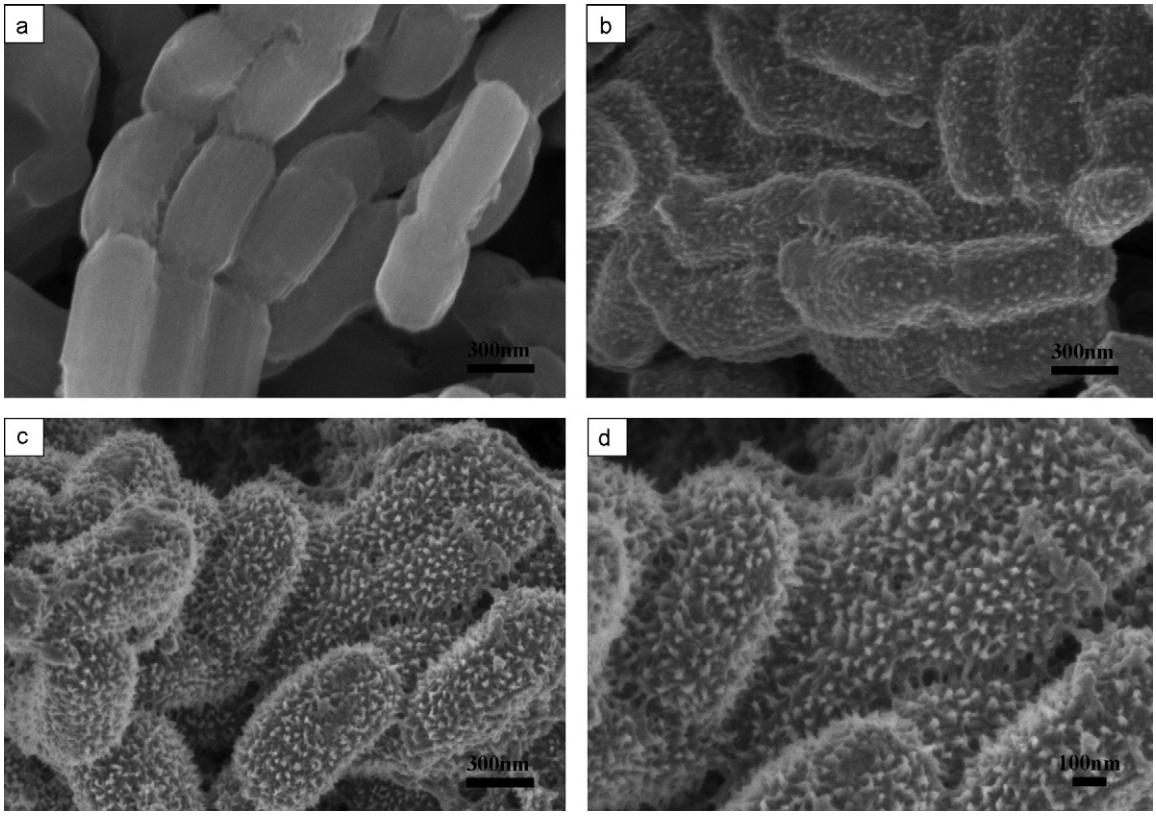

Fig. 2. FE-SEM images of (a) CMK-3, (b) PANI/CMK-3, (c) PANI-NWs/CMK-3; (d) a higher-magnification SEM image of (c).

PANI/CMK-3 nanocomposites was designated as PANI/CMK-3 and PANI-NWs/CMK-3 nanocomposites, respectively in the following passage. Since the mesoporous silica template was removed after the polymerization of aniline monomer, the nanocomposite could preserve the original textural properties from the mesoporous carbon to obtain high surface area.

2.3. Characterization of nanocomposites

X-ray diffraction (XRD) patterns were recorded on a Rigaku D/Max 2550 VB/PC X-ray diffractometer operating at 40 kV and 20 mA using Cu K_α radiation ($\lambda = 0.15406$ nm). Fourier transformation infrared spectra (FTIR) of the samples were measured from KBr sample pellets on a Nicolet 5700 spectrometer. Nitrogen adsorption–desorption isotherms were performed with a ASAP 2020 Micromeritics analyzer at 77 K and the specific surface areas (S_{BET}) were deduced by using the BET equation. The morphology of the final composites was characterized using a HITACHI S4800 field-emission scanning electron microscope (FE-SEM).

2.4. Preparation of electrodes and electrochemical measurement

The working electrodes were prepared by mixing 80 wt% active material, 10 wt% carbon black, and 10 wt% polytetrafluoroethylene (PTFE), then rolled into a thin film with uniform thickness of 0.2 mm, and finally punched into wafers with a geometric surface area of 1 cm^2. Each wafer containing 8 mg active materials was pressed under 1.0×10^7 Pa. Electrochemical experiments were carried out using a teflon swagelok type two-electrode configuration with two stainless-steel sheet as the current collector. Two symmetric working electrodes were sandwiched with a polypropylene (PP) separator and 1 mol L^{-1} aqueous H_2SO_4 was used as an electrolyte. Cyclic voltammetry (CV) experiments were conducted with a PARSTAT 2273/CS130 electrochemical station; galvanostatic charge–discharge (CD) curves and cycle stability were performed with LAND CT2001A at room temperature. The potential range for CV and CD examinations varied from −0.2 V to 0.8 V. The specific capacitance of electrode material was calculated according to the following equation:

$$C = \frac{2(I \times t)}{(m \times \Delta V)}$$

where C is the specific capacitance (F g^{-1}), I is the charge–discharge current (A), t is the discharge time (s), m is the mass of active material within one electrode and $\triangle V$ is the working voltage.

3. Results and discussion

3.1. Morphology and formation mechanism

The morphologies of the pristine CMK-3, PANI/CMK-3 and PANI-NWs/CMK-3 composites were examined by FE-SEM shown in Fig. 2. As one can see from Fig. 2a, the pristine CMK-3 is made of aggregated rod-like particles with smooth surface, while PANI/CMK-3 nanocomposite without CSA shows rough surface due to granular PANI particles deposited on the surface of CMK-3 (Fig. 2b). However, as shown in Fig. 2c, a distinct morphology change of PANI occurs on the external surface of CMK-3 when polymerization is carried out in the presence of CSA. Numerous PANI-NWs grown vertically on the surface of CMK-3 are clearly observed in the PANI/CMK-3 doped with CSA. A higher-magnification SEM image (Fig. 2d) further reveals that PANI-NWs are about 40–50 nm in diameter and 80–100 nm in length.

On the basis of previous reports with PANI nanostructures [27,28], dopant micelles or dopant/aniline salt are proposed as soft template for the formation of PANI-NWs/CMK-3 nanocomposite. Due to the unique amphiphilic structure (hydrophilic $-SO_3H$ and lipophilic $C_{10}H_{15}O-$ group) of CSA, CSA not only serves as a dopant

for PANI but also acts as a surfactant to form micelles during chemical polymerization. Initially, CSA and aniline form CSA/aniline salt due to the acid/base type interactions between the $-SO_3H$ group in CSA and $-NH_2$ group in aniline. Further, the CSA/aniline complex could self-assembly over the surface of SBA-15/carbon composite serving as a hard template through a static interaction to form the micellar structure [29]. When APS is added, the polymerization of aniline only occurs at the micelle/water interface because of hydrophilic APS. Therefore, active nucleation sites of PANI are generated on the outer surface of CMK-3 by heterogeneous nucleation. They can minimize the interfacial energy between the solid surface and bulk solution, which is beneficial to the subsequent growth of PANI on the solid substrates. With the polymerization proceeding, PANI would grow along one dimension instead of forming new nuclei, and eventually aligned PANI-NWs are deposited on the surface of CMK-3.

3.2. Structure characterization

The chemical structure of CMK-3, PANI/CMK-3 and PANI-NWs/CMK-3 was confirmed by FT-IR spectra shown in Fig. 3. Two broad bands at 3424 cm^{-1} and 1132 cm^{-1} are observed in the curve a, which are mainly caused by the stretching vibration of –OH and C–O bonds. As shown in curves b and c, the characteristic peaks at 1578 cm^{-1} and 1494 cm^{-1} can be ascribed to the C=C stretching deformation of quinoid and benzene rings, respectively [30]. Moreover, the characteristic absorption bands in the 1200–1400 cm^{-1} correspond to the C–N stretching band of an aromatic amine. The above bands indicate that PANI chains are formed in both composites.

Fig. 4 presents XRD patterns of CMK-3 and both composites. The XRD of pristine CMK-3 possesses an intense diffraction peak (1 1 0) and two resolved diffraction (1 1 0) and (2 0 0), which could be assigned to the three well-resolved peaks of a highly ordered three dimensional hexagonal mesostructure. Both composites exhibit similar XRD pattern to the CMK-3, except for a slight change in peak intensity. Although CMK-3 surface is functionalized with PANI, the d_{100} spacings for both composites are equivalent to that for CMK-3 at 9.2 nm. It can be concluded that most PANI are selectively located on the surface of CMK-3 particles rather than inside the mesopores.

The structure effects of PANI deposited on the surface of CMK-3 are further illustrated by the N_2 adsorption/desorption isotherm shown in Fig. 5. The isotherms of both composites are typical of type IV and display distinct hysteresis loop at the relative pressure of about 0.4–0.8, which indicate that they are mesoporous materials. The BET surface areas of CMK-3, PANI/CMK-3 and PANI-NWs/CMK-3 are 922, 466 and 497 $m^2 g^{-1}$, respectively. The decrease of the specific area is mainly attributed to the deposition of PANI on the surface of CMK-3. The relatively high surface area of both composites indicates that most mesopores of CMK-3 are effectively preserved after the PANI polymerization completed.

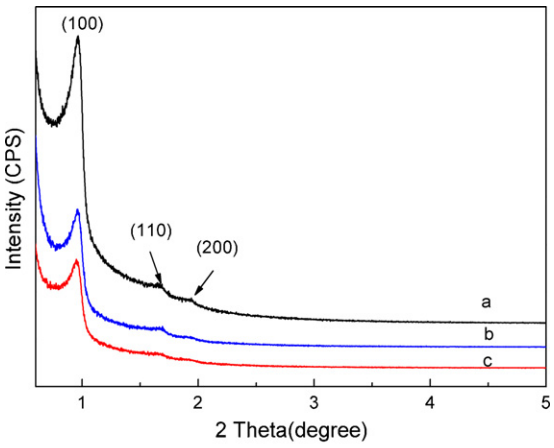

Fig. 4. XRD powder patterns of (a) CMK-3, (b) PANI/CMK-3 and (c) PANI-NWs/CMK-3.

3.3. Electrochemical properties

In order to evaluate the electrochemical performances of the PANI-NWs/CMK-3 nanocomposite, cyclic voltammetry (CV) and galvanostatic charge–discharge tests were performed. Fig. 6a illustrates CV curves for the pure CMK-3 and two composites measured at a scan rate of 20 mV s^{-1} in the potential window of −0.2–0.8 V. The CV shapes of the CMK-3 are almost rectangular without obvious redox peaks, which indicates that CMK-3 mainly possess electrical double-layer capacitance. As for two composites, it can be found that there are two couples of redox peaks in CV curves, attributed to the redox transition of PANI between a semiconducting state (leucoemeraldine form) and a conducting state (polaronic emeraldine form) and the emeraldine–pernigraniline [31]. Furthermore, the current response of the PANI-NWs/CMK-3 nanocomposite is larger than that of the other two materials, implying that it has the highest specific capacitance value. The high specific capacitance of the PANI-NWs/CMK-3 composite mainly derives from the pseudocapacitance of PANI-NWs and partially from electric-double-layer capacitance of CMK-3. The CV curves of the PANI-NWs/CMK-3 composite electrodes are further conducted at different scan rates

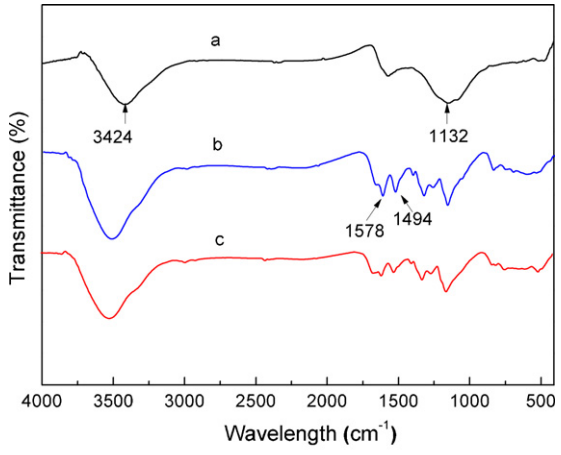

Fig. 3. FTIR spectra of (a) CMK-3, (b) PANI/CMK-3 and (c) PANI-NWs/CMK-3.

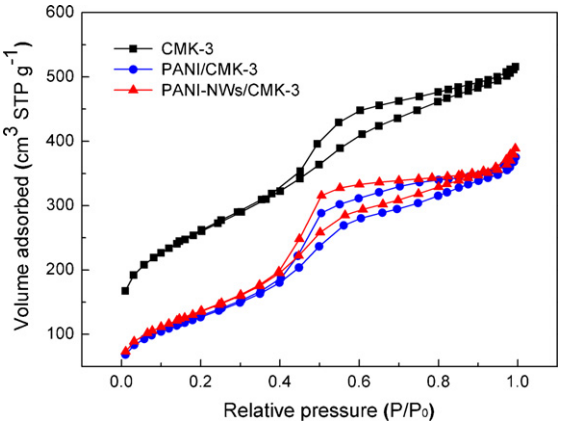

Fig. 5. N_2 adsorption–desorption isotherms of CMK-3, PANI/CMK-3 and PANI-NWs/CMK-3.

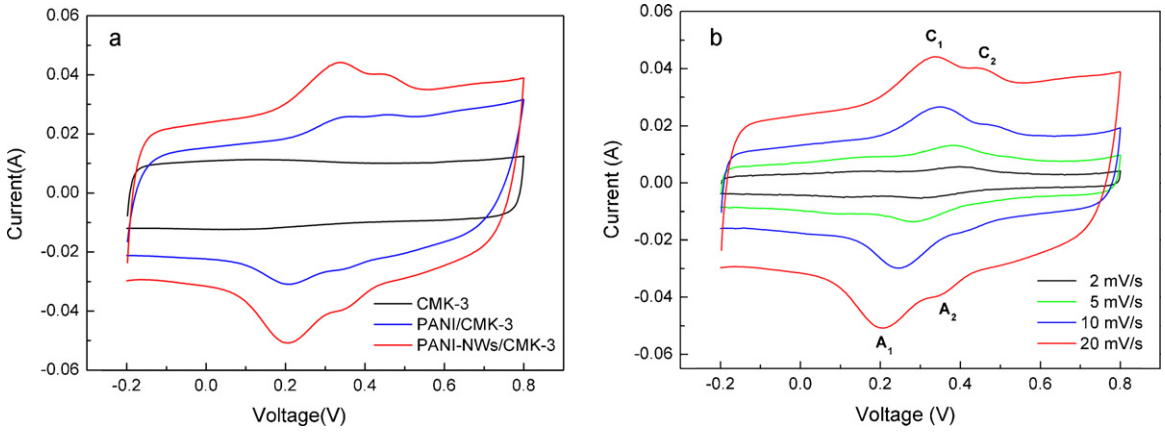

Fig. 6. The cyclic voltammetry within the potential window: (a) CVs of CMK-3, PANI/CMK-3 and PANI-NWs/CMK-3 at 20 mV s^{-1}, (b) CVs of PANI-NWs/CMK-3 composite at different scan rates.

(Fig. 6b). The obvious increase of current with scan rates (e.g., C_1: 0.0055 A at 2 mV s^{-1}, 0.0135 A at 5 mV s^{-1}, 0.0269 A at 10 mV s^{-1} and 0.0442 A at 20 mV s^{-1}) indicates a good rate ability for PANI-NWs/CMK-3 composite.

Fig. 7 presents the galvanostatic charge–discharge curves for three materials measured at a current density of 0.1 A g^{-1}. The supercapacitor based on CMK-3, as an ideal electric double-layer (EDL) capacitor, depicts a typical triangular-shaped curve. Since the existence of PANI in composites, the curve shape is distinct, that is, two clear voltage stages are included: 0.4–0.8 V and −0.2–0.4 V, respectively. During the former, the relatively short charge–discharge duration is ascribed to pure EDL capacitance; the longer charge–discharge duration in the latter stage is the combination of EDL capacitance and faradaic capacitance. The gravimetric capacitance of PANI/CMK-3 and PANI-NWs/CMK-3 (340 F g^{-1} and 470 F g^{-1}) is much higher than CMK-3 (141 F g^{-1}) at a current density of 0.1 A g^{-1}, indicating the synergic effect of PANI and CMK-3, which is in agreement with the result of the CV curves.

It is notable that the PANI-NWs/CMK-3 electrode has higher capacity than PANI/CMK-3 at various current densities (Fig. 8). The synthesis procedure and the amount of aniline monomer to CMK-3 in two composites are the same, except for the addition of CSA during the preparation of PANI-NWs/CMK-3 composite. Therefore, it can be concluded that the enhanced electrochemical performance is mainly attributed to the vertically aligned PANI nanowhisker arrays on the outer surface of CMK-3. The advantage of this unique morphology is that it can facilitate the ion diffusion from the electrolyte to the surface of the active materials in a short time. Meanwhile, the small PANI-NWs can shorten the charge transfer distance, which ensure the high utilization of PANI [20,32]. On the other hand, the retained high surface area of the PANI-NWs/CMK-3 composite also plays an important role in the excellent electrochemical performance due to numerous highly conductive paths provided by CMK-3. The capacitance retention of PANI-NWs/CMK-3 composite is 87% as current densities increase from 0.1 A g^{-1} to 2 A g^{-1}, whereas that of PANI/CMK-3 is only 75% under similar experiments. The result indicates the PANI-NWs/CMK-3 composite electrode has better rate capability.

The cycling stability of CMK-3 and PANI-NWs/CMK-3 electrodes was measured by charge–discharge cycling at a current density of 1 A g^{-1}, as shown in Fig. 9. The specific capacitance of pure CMK-3 retains almost 100% after 1000 charge–discharge cycles. However, the PANI-NWs/CMK-3 electrode shows a slight decrease during first 200 cycles and subsequently keeps stable. Apparently, the final capacitance of PANI-NWs/CMK-3 composite is much higher than pure CMK-3. Recent studies indicate that pure PANI as electrode materials shows low capacitance retention [23,24]. However, in our experiment, the capacitance retention of the PANI-NWs/CMK-3 composite electrode keeps 90.4% after 1000 charge–discharge cycles. This result demonstrates that the improved cycling stability may come from the synergistic effect of PANI-NWs and CMK-3. The ordered CMK-3 framework prevents PANI from severely swelling and shrinking during the charge–discharge process; while facile strain relaxation in the vertical PANI-NW arrays can effectively

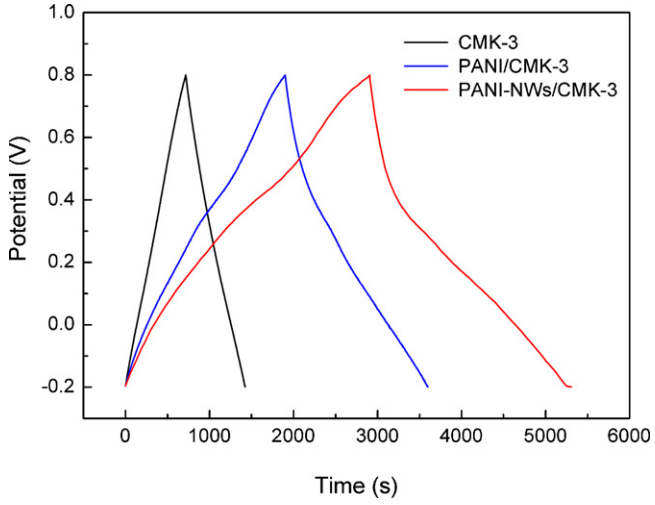

Fig. 7. Galvanostatic charge–discharge curves of CMK-3, PANI/CMK-3, PANI-NWs/CMK-3 at a current density of 0.1 A g^{-1}.

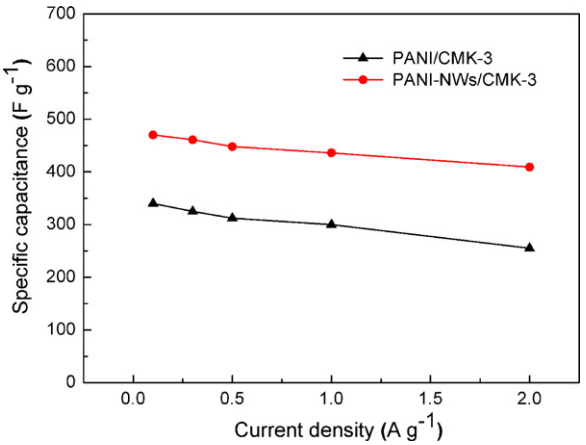

Fig. 8. Specific capacitance of PANI/CMK-3 and PANI-NWs/CMK-3 at different current densities.

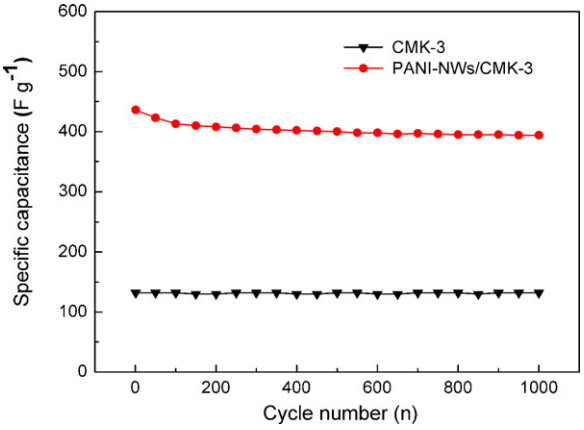

Fig. 9. Cycling performance of CMK-3 and PANI-NWs/CMK-3 under a current density of 1 A g^{-1}.

reduce the breaking of PANI chains during the doping/dedoping process of counterions [33,34]. Therefore, the PANI-NWs/CMK-3 nanocomposite shows a good cycling stability.

4. Conclusions

A facile strategy was developed to synthesize PANI-NWs/CMK-3 nanocomposites on the premise of preserving the mesopore paths of CMK-3. PANI-NWs were completely formed prior to the removal of mesoporous silica templates and this synthetic procedure could obtain the composite with high surface area (497 m^2 g^{-1}). The existence of CSA results in vertically aligned PANI-NW arrays uniformly distributed on the outer surface of CMK-3 particles. Supercapacitor devices based on this nanocomposite with 40 wt% PANI possessed a large specific capacitance (470 F g^{-1}) at a current density of 0.1 A g^{-1}. The synergistic effect of small nanosized PANI arrays and well-ordered mesoporous carbon endows the composite with high electrochemical capacitance and good cycling stability. Therefore, design and fabrication of one-dimensional conducting polymer on carbon materials are expected to be a meaningful research direction for electrode materials in supercapacitors.

Acknowledgements

This work was supported by the National Natural Science Foundation of China (20925621), the Special Projects for Nanotechnology of Shanghai (1052nm02300, 0952nm02000, 0952nm02100), the Shanghai Pujiang Program (09PJ1403200), the Fundamental Research Funds for the Central Universities (WD1013014), the Program of Shanghai Subject Chief Scientist (08XD1401500) and the Special Projects for Key Laboratories in Shanghai (10DZ2211100).

References

[1] M. Winter, R.J. Brodd, Chem. Rev. 104 (2004) 4245.
[2] B.E. Conway, J. Electrochem. Soc. 138 (1991) 1539.
[3] K.H. An, W.S. Kim, Adv. Funct. Mater. 11 (2001) 387.
[4] D.W. Wang, F. Li, M. Liu, G.Q. Lu, H.M. Cheng, Angew. Chem. Int. Ed. 47 (2008) 373.
[5] P. Simon, Y. Gogotsi, Nat. Mater. 7 (2008) 845.
[6] F. Montilla, M.A. Cotarelo, E. Morallon, J. Mater. Chem. 19 (2009) 305.
[7] K.S. Ryu, K.M. Kim, N.G. Park, Y.J. Park, S.H. Chang, J. Power Sources 103 (2002) 305.
[8] Z. Lei, H. Zhang, S. Ma, Y. Ke, J. Li, F. Li, Chem. Commun. 7 (2002) 676.
[9] S. Jun, S.H. Joo, R. Ryoo, M. Kruk, M. Jaroniec, Z. Liu, T. Ohsuna, O. Terasaki, J. Am. Chem. Soc. 122 (2000) 10712.
[10] L.X. Li, H.H. Song, X.H. Chen, Electrochim. Acta 51 (2006) 5715.
[11] A.B. Fuertes, G. Lota, T.A. Centeno, E. Frackowiak, Electrochim. Acta 50 (2005) 2799.
[12] D.W. Wang, F. Li, H.T. Fang, M. Liu, G.Q. Lu, H.M. Cheng, J. Phys. Chem. B 110 (2006) 8570.
[13] S. Yoon, J. Lee, T. Hyeon, S.M. Oh, J. Electrochem. Soc. 147 (2000) 2507.
[14] C.H. Kim, S.-S. Kim, F. Guo, T.P. Hogan, T.J. Pinnavaia, Adv. Mater. 16 (2004) 736.
[15] W. Xing, S.P. Shu, H.Y. Cui, Z.F. Yan, Mater. Lett. 61 (2007) 4627.
[16] L.X. Li, H.H. Song, Q.C. Zhang, J.Y. Yao, X.H. Chen, J. Power Sources 187 (2009) 268.
[17] S.M. Zhu, J.J. Gu, Z.X. Chen, J.P. Dong, X.Y. Liu, C.X. Chen, D. Zhang, J. Mater. Chem. 20 (2010) 5123.
[18] J. Zhang, L.B. Kong, J.J. Cai, Y.C. Luo, L. Kang, Electrochim. Acta 55 (2010) 8067.
[19] Y.Q. Dou, Y.P. Zhai, H.J. Liu, Y.Y. Xia, B. Tu, D.Y. Zhao, X.X. Liu, J. Power Sources 196 (2011) 1608.
[20] Y.G. Wang, H.Q. Li, Y.Y. Xia, Adv. Mater. 18 (2006) 2619.
[21] A.S. Arico, P. Bruce, B. Scrosati, J.M. Tarascon, Nat. Mater. 4 (2005) 366.
[22] A. Malinauskas, J. Malinauskiene, A. Ramanavicius, Nanotechnology 16 (2005) R51.
[23] B.K. Kuila, B. Nandan, M. Bohme, A. Janke, M. Stamm, Chem. Commun. (2009) 5749.
[24] J.J. Xu, K. Wang, S.Z. Zu, B.H. Han, Z.X. Wei, ACS Nano 4 (2010) 5019.
[25] D.Y. Zhao, J.L. Feng, Q.S. Huo, N. Melosh, G.H. Fredrickson, B.F. Chmelka, G.D. Stucky, Science 279 (1998) 548.
[26] Y.S. Choi, S.H. Joo, S.-A. Lee, D.J. You, H. Kim, C. Pak, H. Chang, D. Seung, Macromolecules 39 (2006) 3275.
[27] L.J. Zhang, M.X. Wan, Nanotechnology 13 (2002) 750.
[28] N.R. Chiou, C.M. Lu, J.J. Guan, L.J. Lee, A.J. Epstein, Nat. Nanotechnol. 2 (2007) 354.
[29] X. Li, M.X. Wan, Y. Wei, J.Y. Shen, Z.J. Chen, J. Phys. Chem. B 110 (2006) 14623.
[30] A.P. Monkman, P. Adams, Synth. Met. 40 (1991) 87.
[31] C.C. Hu, J.Y. Lin, Electrochim. Acta 47 (2002) 4055.
[32] K. Wang, J.Y. Huang, Z.X. Wei, J. Phys. Chem. C 114 (2010) 8062.
[33] Z.B. Lei, Z.W. Chen, X.S. Zhao, J. Phys. Chem. C 114 (2010) 19867.
[34] J.Y. Huang, K. Wang, Z.X. Wei, J. Mater. Chem. 20 (2010) 1117.